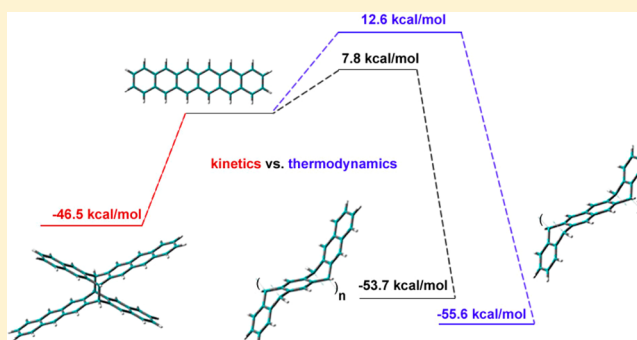


# Formation of Acene-Based Polymers: Mechanistic Computational Study

Natalia Zamoshchik,<sup>\*,†</sup> Sanjio S. Zade,<sup>\*,‡</sup> and Michael Bendikov<sup>†,§</sup><sup>†</sup>Department of Organic Chemistry, Weizmann Institute of Science, Rehovot 76100, Israel<sup>‡</sup>Department of Chemical Sciences, Indian Institute of Science Education and Research, Kolkata, P.O. BCKV Campus Main Office, Mohanpur 741252, Nadia, West Bengal, India

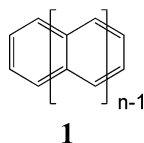
## Supporting Information

**ABSTRACT:** Understanding the mechanism of linear acene decomposition and its reactivity is a prerequisite for controlling the stability of acenes and their future applications. Previously, we suggested that long acenes may undergo polymerization since the polymerization product is thermodynamically more stable than the dimerization product. However, due to kinetic considerations, the most thermodynamically stable product, the polymer, might not necessarily be formed. To elucidate the situation, we investigated the mechanisms of acene polymerization computationally, using pentacene, hexacene, and heptacene as representative examples. Similarly to dimerization, acene polymerization follows a stepwise biradical pathway. Structural and steric hindrance of the polymer backbone forces acene polymerization to proceed via the less reactive noncentral benzene rings. Consequently, dimerization is always kinetically more favorable than polymerization, irrespective of acene length. Although, for long acenes starting from hexacene, both polymerization and dimerization are barrierless pathways relative to the reactants, polymerization is thermodynamically preferred for hexacene and heptacene and even more so for longer acenes (since polymerization forms four new C–C bonds while dimerization forms only two). Indeed, reinvestigation of available experimental data suggests that acene-based polymers were probably obtained experimentally previously.



## INTRODUCTION

Acenes (**1**),<sup>1</sup> which consist of linearly fused benzene rings, are of great interest to the broad materials science and engineering communities.<sup>2</sup> The good semiconducting properties of pentacene have led to considerable research into its application in field-effect transistors (FETs) and have stimulated interest in the synthesis of longer acenes.<sup>2–4</sup> These efforts have born fruit during the past decade, with the synthesis of hexacenes, octacenes, and nonacenes.<sup>5–7</sup> Acenes are also of fundamental interest as a general model for long conjugated systems. Thus, basic understanding of acene reactivity is very important for the development of organic electronic devices comprising these molecules and for understanding the reactivity of long  $\pi$ -conjugated systems.<sup>8,9</sup>



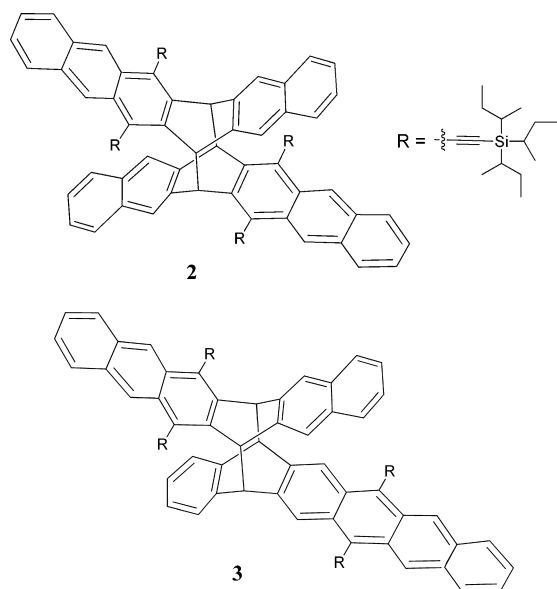
The photoreactivity,<sup>10</sup> including photodimerization, of acenes is widely known, but their thermal reactions are less understood.<sup>11</sup> Anthony's group has reported that hexacene with bulky substituents can undergo dimerizations via both thermal

and photochemical pathways.<sup>12</sup> Under ambient laboratory lightening, formation of a symmetrical dimer (**2**) was observed. However, in the absence of light, dimer (**3**) was observed as a thermal dimerization product. The change in the regiochemistry of dimerization was explained in terms of the orientation of the starting monomer in the solid state. Wudl's group<sup>13</sup> discovered that 2,3,9,10-tetrachloropentacene could produce poly(iptycene) via a Diels–Alder self-coupling reaction.

Recently, we have reported a computational study of the thermal dimerization of acenes,<sup>14</sup> which can be viewed as a formally thermally symmetry-forbidden [4 + 4] reaction. We explored the mechanism of dimerization for benzene, naphthalene, anthracene, pentacene, and heptacene. Benzene and naphthalene dimerize only via a concerted asynchronous pathway; however, anthracene and pentacene prefer a multistep biradical mechanism. In heptacene, the complex formed by two heptacene molecules collapses in a multistep dimerization process to form the product.<sup>14</sup> The activation barriers for thermal dimerization decrease rapidly with increasing acene chain length and are calculated (at M06-2X/6-31G(d)+ZPVE) to be 77.9, 57.1, 33.3, –0.3, and –12.1 kcal/mol vs two isolated

Received: March 26, 2013

Published: September 23, 2013



acene molecules for benzene, naphthalene, anthracene, pentacene, and heptacene, respectively.<sup>14</sup> We also suggested the formation of an acene-based polymer as an alternative favorable route for the dimerization of longer acenes (hexacene onward); however, we only studied the thermodynamics of the formation of the acene-based polymers in ref 14. In the absence of information on the kinetics of acene polymerization and without knowing the structures of the preferably formed polymers, it is not possible to assess the feasibility of acene polymerization based on our previous work.<sup>14</sup>

Acene-based polymers were reported in an outstanding PhD thesis<sup>15</sup> (supervised by Chapman). More recently, the Neckers and Bettinger groups reported the formation and decomposition of unsubstituted heptacene.<sup>5c</sup> Examination of the UV–vis spectrum<sup>5c</sup> they obtained after annealing photogenerated heptacene in an Ar matrix reveals the formation of a product comprising naphthalene units and not anthracene units. This may suggest<sup>14</sup> the formation of acene-based polymers, such as **poly-7P-3,3'** or other similar polymers, rather than the formation of the heptacene dimer **7P-4,4'**, which has anthracene units (Figure 1). Thus, it should be considered that acenes might not only dimerize but also undergo other self-reactions, such as polymerization. Unfortunately, it is very difficult to distinguish between the products of dimerization vs polymerization of long acenes using experimental tools as both should be practically insoluble and produce similar solid-state

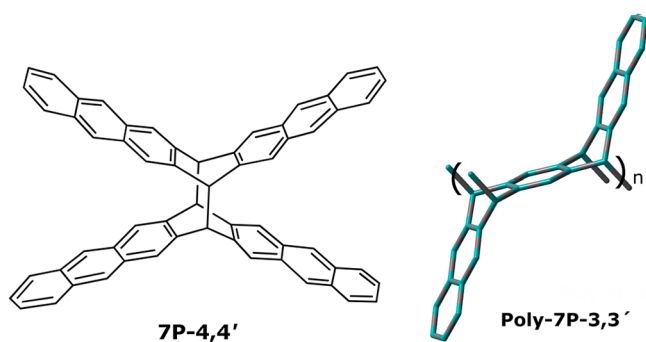


**Figure 1.** (Left) heptacene dimerization product **7P-4,4'**. (Right) heptacene polymerization product **poly-7P-3,3'**.

<sup>13</sup>C NMR spectra. Thus, computational techniques are the only practical means available for studying acene self-reactivity and understanding acene polymerization.

In the present computational study, we explored the mechanism (kinetics) of acene polymerization for pentacene, hexacene, and heptacene. For acenes of any length, dimerization is always kinetically more favorable than polymerization, as dimerization proceeds through the more reactive central rings. However, for hexacene and higher acenes, polymerization to produce an acene-based polymer is significantly favored thermodynamically over the usual dimerization. In some cases, the formation of thermodynamically preferred polymers is highly unlikely because of the steric requirements of the polymerization process. Nevertheless, on the basis of our computational results, the formation of acene based polymers is one of the possible reactions or decomposition pathways of long acenes.

## COMPUTATIONAL METHODS

The Gaussian 09<sup>16</sup> series of programs was used for all computations. The molecules were fully optimized using density functional theory<sup>17</sup> at the M06-2X level,<sup>18</sup> and since the studied systems are quite large, the economical basis set 6-31G(d) was used (denoted as M06-2X/6-31G(d)). In our previous paper,<sup>14</sup> we showed that the M06-2X functional is very suitable for studying the kinetics and thermodynamics of acene dimerization. At the M06-2X/6-31G(d) level, the hexacene molecule does not show biradical character and the restricted wave function is stable, while heptacene and longer acenes exhibit biradical character and the restricted wave function is unstable. When the restricted wave function was unstable, calculations were performed using the broken-symmetry unrestricted DFT (UDFT) method, and the species were optimized at the UM06-2X/6-31G(d) level of theory. Spin contamination ( $\langle S^2 \rangle$ ) values reported in this paper are without spin annihilation. Frequency calculations were performed at the M06-2X/6-31G(d) level for all stationary points of finite size molecules. Intrinsic reaction coordinate (IRC)<sup>19</sup> calculations were performed for several representative cases. Unscaled zero point vibrational energies (ZPVE) at the M06-2X/6-31G(d) level were added to the calculated relative energies. Gibbs free energies ( $\Delta G$ ) were calculated at 298 K and 1 atm at the M06-2X/6-31G(d) level. The calculations for polymers were performed using the periodic boundary conditions (PBC) approximation as implemented in Gaussian 09.<sup>20</sup> Since frequency calculations cannot be performed within a PBC approximation, ZPVE were not calculated for polymers and were not added to their reactive energies.

The polymerization mechanism was calculated by modeling a single propagation polymerization step and by considering only one acene unit in the backbone. The terminal unit of the polymer was constructed by adding two hydrogen atoms onto the reacting acenes engaged in backbone formation (Figure 2).<sup>21</sup> The mechanism of addition of the next acene molecule to such an acene unit was calculated.

We use the following nomenclature in this paper. 7-2H-2 and 7-2H-3 indicate heptacene dihydrogens (Figure 2) in which the additional hydrogens are on the second and third rings, respectively. In complexes between a polymer and an additional acene molecule, -2<sub>3</sub> indicates that two hydrogens were placed on the second benzene ring of the polymer and that the additional acene molecule is positioned in front of the third benzene ring of the polymer. In the intermediates such as **6M<sub>in</sub>-42** and **6M<sub>in</sub>**, the subscript indicates an “in” type minimum for the polymerization of hexacene, and -42 indicates the involvement of the fourth benzene ring of the acene unit in the forming polymer and the second benzene ring of the additional hexacene molecule. Similar nomenclature is used for all transition states, minima, and products.

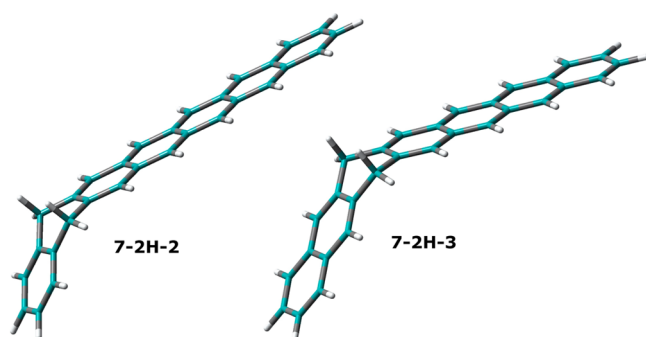


**Figure 2.** Modeling of the polymer terminal unit by placing two additional hydrogen atoms on the second benzene ring of the heptacene molecule 7-2H-2 or on the third benzene ring of the heptacene molecule 7-2H-3.

## RESULTS AND DISCUSSION

At the M06-2X/6-31G(d) level of theory, pentacene dimerization to form the most stable dipentacene (**5P-3,3'**, Table 1 and Figure 3) is 2.1 kcal/mol more favorable than the

**Table 1.** Calculated Energies of Acene Dimers and Polymers Shown in Figures 3 and 4 (Relative to the Two Molecules of the Respective Ground-State Acenes, in kcal/mol, at M06-2X/6-31G(d) without Inclusion of ZPVE)<sup>a</sup>

	$\Delta E$	$\Delta\Delta E^b$		$\Delta E$	$\Delta\Delta E^b$
<b>5P-3,3'</b> <sup>c</sup>	-39.1		<b>6P<sub>trans</sub></b> <sup>c</sup>	-46.5	
<b>poly-5P-2,2'</b> <sup>c</sup>	-37.0	2.1	<b>poly-6P-2,3'</b> <sup>c,22</sup>	-53.7	-7.2
<b>poly-5P-3,1'</b>	10.9	50.1	<b>poly-6P-2,2'</b> <sup>c</sup>	-55.6	-9.1
<b>7P-4,4'</b> <sup>c</sup>	-54.2		<b>poly-6P-2,3'-alt-2,2'</b>	-54.7	-8.2
<b>poly-7P-3,3'</b> <sup>c,d</sup>	-71.0	-16.8	<b>8P<sub>trans</sub></b> <sup>c</sup>	-55.0	
<b>poly-7P-2,3'</b>	-72.6	-18.4	<b>poly-8P-3,3'</b> <sup>c</sup>	-86.5	-31.5

<sup>a</sup>For heptacene and octacene, the energies of the reactants were calculated at UM06-2X/6-31G(d). <sup>b</sup> $\Delta\Delta E = \Delta E$  (polymer) -  $\Delta E$  (dimer). Two polymer unit cells were used for the energy calculations. <sup>c</sup>From ref 14. <sup>d</sup>Formation of this polymer is unlikely from a kinetic point of view because of the steric requirements of the polymerization process.

formation of the most stable pentacene-based polymer (**poly-5P-2,2'**, Table 1 and Figure 4)<sup>14</sup> and 50.1 kcal/mol more favorable than the formation of **poly-5P-3,1'**. However, some of the acene-based polymers obtained from hexacene onward are more stable than the corresponding dimers (Table 1), which shows that the formation of acene-based polymers from long oligoacenes is thermodynamically preferred over dimerization. Consequently, competition between the formation of dimers and acene-based polymers shifts toward the formation

of polymers as acene chain length increases.<sup>14</sup> However, as we will discuss below, in some cases the formation of the most thermodynamically preferred polymers is highly unlikely because of steric effects along the reaction pathway. Thus, in order to understand and predict the formation of acene-based polymers vs formation of acene dimers, a more detailed investigation was performed.

In this work, we performed a comprehensive study of the polymerization of pentacene, hexacene, and heptacene. Hexacene polymers **poly-6P-2,2'**, **poly-6P-2,3'-alt-2,2'**, and **poly-6P-2,3'** are 9.1, 8.2, and 7.2 kcal/mol, respectively, more stable than the corresponding dimer **6P<sub>trans</sub>** (Table 1 and Figures 3 and 4). Thus, the formation of hexacene based polymers is thermodynamically preferred over dimerization. **Poly-7P-3,3'** and **poly-7P-2,3'** are 71.0 and 72.6 kcal/mol, respectively, more stable than two heptacene molecules and are 16.8 and 18.4 kcal/mol, respectively, more stable than the most stable dimer **7P-4,4'**. Importantly, the formation of **poly-7P-2,3'** should be significantly preferred over that of **poly-7P-3,3'** in view of the reaction kinetics (see below). The formation of the octacene based polymer **poly-8P-3,3'** is favored over the formation of the dimer **8P<sub>trans</sub>** by as much as 31.5 kcal/mol. Thus, from a thermodynamic point of view, the formation of acene-based polymers for long acenes is much more preferable than dimerization.

**Polymerization Mechanism. a. General Considerations.** Polymerization of an acene requires the addition of an acene molecule to the backbone, which contains  $sp^3$  carbons formed by previously added acene molecules. Compared to the pristine acene, the terminal unit of the polymer consists of shorter and less reactive acene fragments since part of its backbone is interrupted by  $sp^3$  carbons. The presence of  $sp^3$  carbons causes the terminal unit to curve and prevents polymerization via rings adjacent to the  $sp^3$  unit. Thus, acene polymerization involves the approaching acene effectively reacting with a shorter acene, rather than with one of equal length (as in dimerization). Steric considerations also dictate that the addition of new acene molecules during polymerization proceeds only in a *syn*-fashion (with the acene molecules facing and maximally overlapping each other). The addition of acene in an *anti*-fashion (in which the approaching acene molecule is shifted relative to the second acene molecule or terminal unit of the polymer backbone, so that there is little overlap between the two molecules) would require the approaching molecule to undergo a nearly 180° rotation to form the product, which is not sterically possible (see, for example, Figure 5 below). Therefore, following formation of a complex, the reaction should proceed directly to the product via a *syn*-transition state ( $T_{in}$ ) followed by a *syn*-minimum ( $M_{in}$ ) and another transition state ( $T_{form}$ ), similar to the pathway calculated for the dimerization of pentacene by a biradical stepwise mechanism.<sup>14</sup>

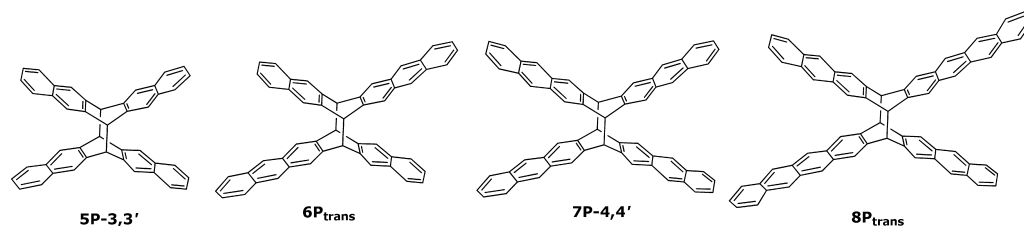


**Figure 3.** Representative structures of dimerization products (**P**). The first digit refers to the number of fused benzene rings in the corresponding acene monomer.

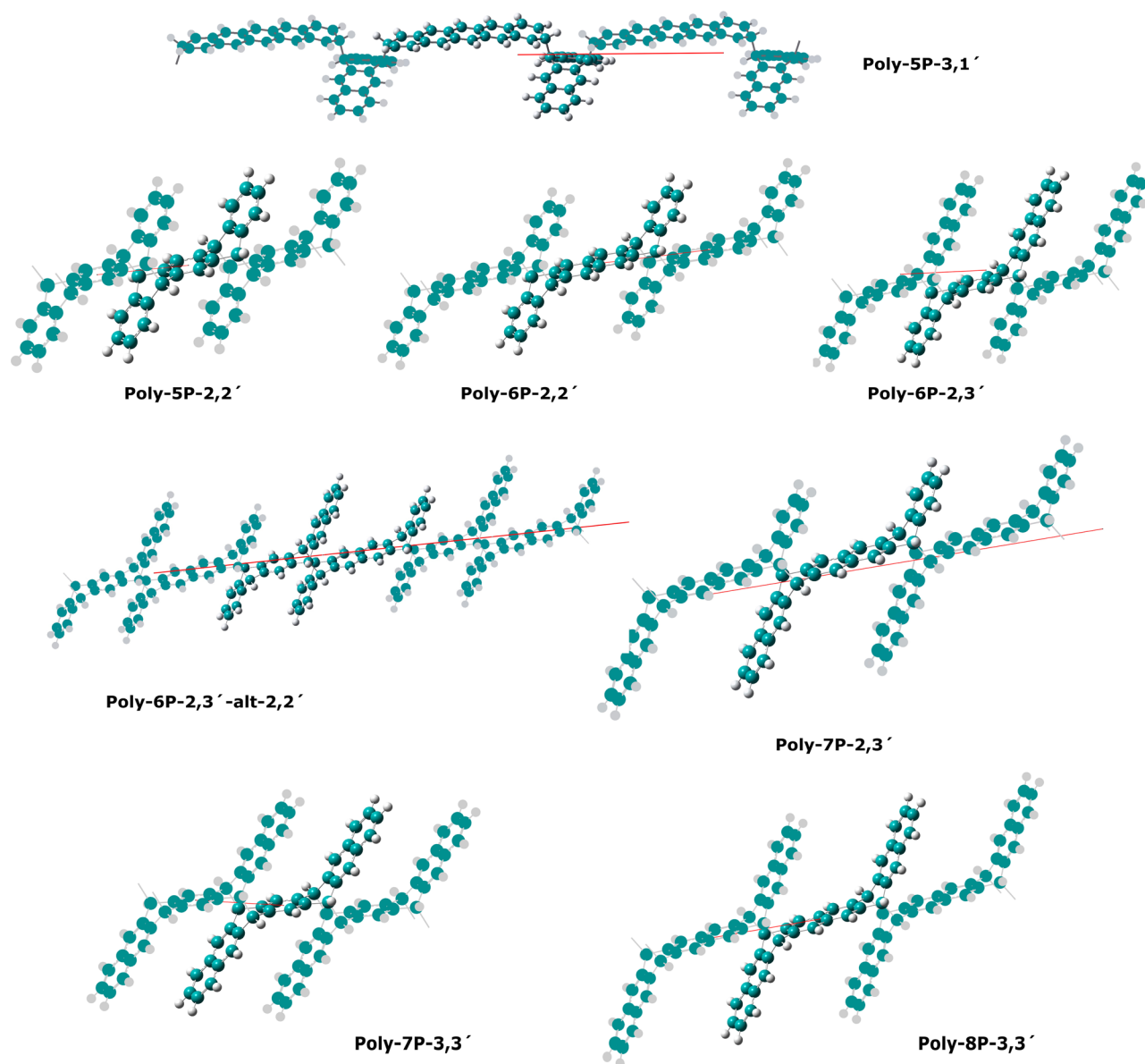


**Figure 4.** Representative optimized structures (PBC/M06-2X/6-31G(d)) of the acene-based polymers. Main unit cell atoms are shown using a ball-and-stick representation, and atoms in replicated unit cells are shown using a blunt representation. The red line shows the direction of the unit cell vector.

During polymerization, each acene molecule forms four new C–C bonds with the neighboring two molecules, whereas during dimerization, only two such C–C bonds are formed for each acene molecule. In the calculated polymerization mechanism, the thermodynamics is calculated for the addition of one molecule (one mole) of acene, but for dimerization, the reaction energies are calculated per two acene molecules (two moles). Consequently, the thermodynamics of acene polymerization (given in Table 2 and Figures 5–13) should be compared with twice the dimerization energies (given in Table 1). For example, the energies of formation of polymers **poly-6P-2-2'** (–55.6 kcal/mol, per two acene molecules) and **poly-7P-2-3'** (–72.6 kcal/mol, per two acene molecules) are nearly double the energy of formation of the corresponding product of the propagation step **6P-53** (–30.5 kcal/mol) and **7P-63** (–31.2 kcal/mol), respectively (Tables 1 and 2).

*b. Polymerization of Pentacene.* For the polymerization of pentacene, we have considered a mechanism starting from **5-**

**complex-2<sub>3</sub>**, which will lead to the addition of pentacene via its second ring to the second ring of the anthracene unit of the polymeric backbone (Figure 5).<sup>21</sup> Polymerization proceeding via this complex should lead to the most preferred polymerization pathway for pentacene. The formation of **5-complex-2<sub>3</sub>** is exothermic by 14.3 kcal/mol, which is less exothermic than the formation of a complex between two pentacene molecules (–17.0 kcal/mol<sup>14</sup>). **5-Complex-2<sub>3</sub>** can be compared with a complex between an anthracene and a pentacene molecule in which only three benzene rings overlap. Polymerization proceeding via **5-complex-2<sub>3</sub>** will lead to the formation of **poly-5P-2,2'**, which is 37.0 kcal/mol more stable than two starting pentacene molecules (Table 1). From a mechanistic point of view, from **5-complex-2<sub>3</sub>** the reaction proceeds via **5T<sub>in</sub>-42**, whose activation energy lies 11.0 kcal/mol higher than the reactants, to form a new minimum, **5M<sub>in</sub>-42**, at 9.2 kcal/mol above the reactants. **5M<sub>in</sub>-42** leads to the propagation step product **5P-42** via the rate-determining step **5T<sub>form</sub>-42** with

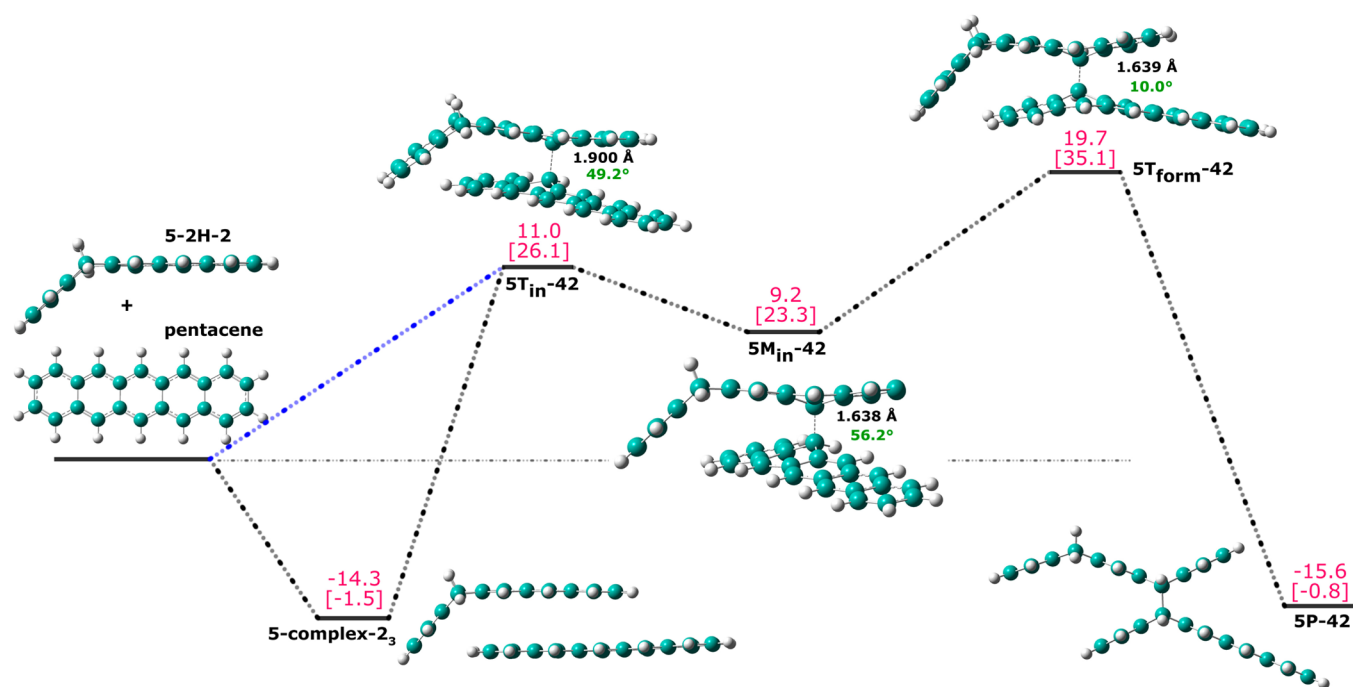


**Figure 5.** Reaction path for a propagation step in pentacene polymerization starting from the **5-complex-2<sub>3</sub>** at M06-2X/6-31G(d)+ZPVE. This reaction should lead to formation of the polymer **poly-SP-2,2'** (Figure 4). Calculated energies (in kcal/mol, red), bond lengths (in Å, black), and dihedral angles (green) of newly forming C–C bonds (dashed lines between molecules) are shown. The Gibbs free energy ( $\Delta G$ , in kcal/mol) values are given in brackets.<sup>21</sup>

**Table 2.** Calculated Energies ( $\Delta E$ ) and the Gibbs Free Energies ( $\Delta G$ ) of the Complexes, Transition States (T), Local Minima (M), and Products (P) (Relative to the Respective Ground State Acene and Appropriate Dihydrogen–Acene, in kcal/mol) at M06-2X/6-31G(d)+ZPVE for the Propagation Step in the Polymerization of Pentacene, Hexacene, and Heptacene<sup>a,b</sup>

	$\Delta E$	$\Delta G$		$\Delta E$	$\Delta G$
pentacene polymerization			hexacene dimerization		
<b>5-complex-2<sub>3</sub></b>	-14.3 (-14.8)	-1.5	<b>6-complex</b>	-19.3 (-20.4)	-5.4
<b>5T<sub>in</sub>-42</b>	11.0 (10.8)	26.1	<b>6T<sub>in</sub></b>	-7.0 (-7.1)	6.7
<b>5M<sub>in</sub>-42</b>	9.2 (8.1)	23.3	<b>6M<sub>in</sub></b>	-15.8 (-17.8)	-2.8
<b>5T<sub>form</sub>-42</b>	19.7 (19.1)	35.0	<b>6T<sub>form</sub></b>	-10.6 (-12.6)	5.0
<b>5P-42</b>	-15.6 (-19.6)	-0.8	<b>6P<sub>trans</sub></b>	-41.8 (-46.5)	-26.3
hexacene polymerization			heptacene polymerization <sup>b</sup>		
<b>6-complex-2<sub>3</sub></b>	-17.2 (-18.3)	-3.0	<b>7-complex-2<sub>3</sub></b>	-20.8 (-22.0)	-2.6
<b>6T<sub>in</sub>-42</b>	3.6 (3.1)	19.7	<b>7T<sub>in</sub>-53</b>	-8.3 (-9.4)	8.3
<b>6M<sub>in</sub>-42</b>	-0.1 (-0.9)	14.4	<b>7M<sub>in</sub>-53</b>	-14.2 (-16.8)	1.4
<b>6T<sub>form</sub>-42</b>	7.8 (6.7)	24.8	<b>7P-53</b>	-38.6 (-44.4)	-23.3
<b>6P-42</b>	-23.9 (-28.1)	-9.6	<b>7-complex-2<sub>4</sub></b>	-17.3 (-17.1)	-0.6
<b>6T<sub>in</sub>-53</b>	0.2 (-0.1)	15.1	<b>7T<sub>in</sub>-52</b>	-1.7 (-1.3)	15.1
<b>6M<sub>in</sub>-53</b>	-4.7 (-5.8)	10.3	<b>7M<sub>in</sub>-52</b>	-6.2 (-9.0)	0.0
<b>6T<sub>form</sub>-53</b>	1.5 (0.3)	18.3	<b>7T<sub>form</sub>-52</b>	1.9 (-0.7)	17.8
<b>6P-53</b>	-30.5 (-34.9)	-15.9	<b>7P-52</b>	-31.2 (-36.9)	-15.8
<b>6-complex-2<sub>4</sub></b>	-12.5 (-13.6)	0.5	<b>7-complex-3<sub>4</sub></b>	-18.0 (-18.4)	-1.2
<b>6T<sub>in</sub>-52</b>	6.3 (6.4)	21.1	<b>7T<sub>in</sub>-63</b>	-0.5 (-2.0)	15.2
<b>6M<sub>in</sub>-52</b>	1.7 (0.3)	16.2	<b>7M<sub>in</sub>-63</b>	-5.0 (-8.5)	10.1
<b>6T<sub>form</sub>-52</b>	12.6 (11.7)	26.8	<b>7T<sub>form</sub>-63</b>	0.3 (-2.3)	17.3
<b>6P-52</b>	-24.2 (-28.4)	-9.5	<b>7P-63</b>	-31.2 (-36.9)	-15.7
<b>6-complex-3<sub>4</sub></b>	-14.2 (-14.8)	-0.9			
activation energies for dimerization <sup>14</sup>					
<b>5T<sub>form</sub></b>	-0.3 (-1.5)	16.1	<b>7T<sub>1</sub></b>	-12.1 (-14.6)	6.3

<sup>a</sup>Values in parentheses are without ZPVE (to enable comparison with the polymerization energies given in Table 1). <sup>b</sup>The energies of the reactants and complexes for heptacene polymerization, which have biradical character, were calculated at UM06-2X/6-31G(d).

activation energy of 19.7 kcal/mol relative to the starting materials (cf., an activation energy for pentacene dimerization

of -0.3 kcal/mol relative to the starting materials<sup>14</sup>). Formation of **5P-42** is exothermic by 15.6 kcal/mol (19.6 kcal/mol

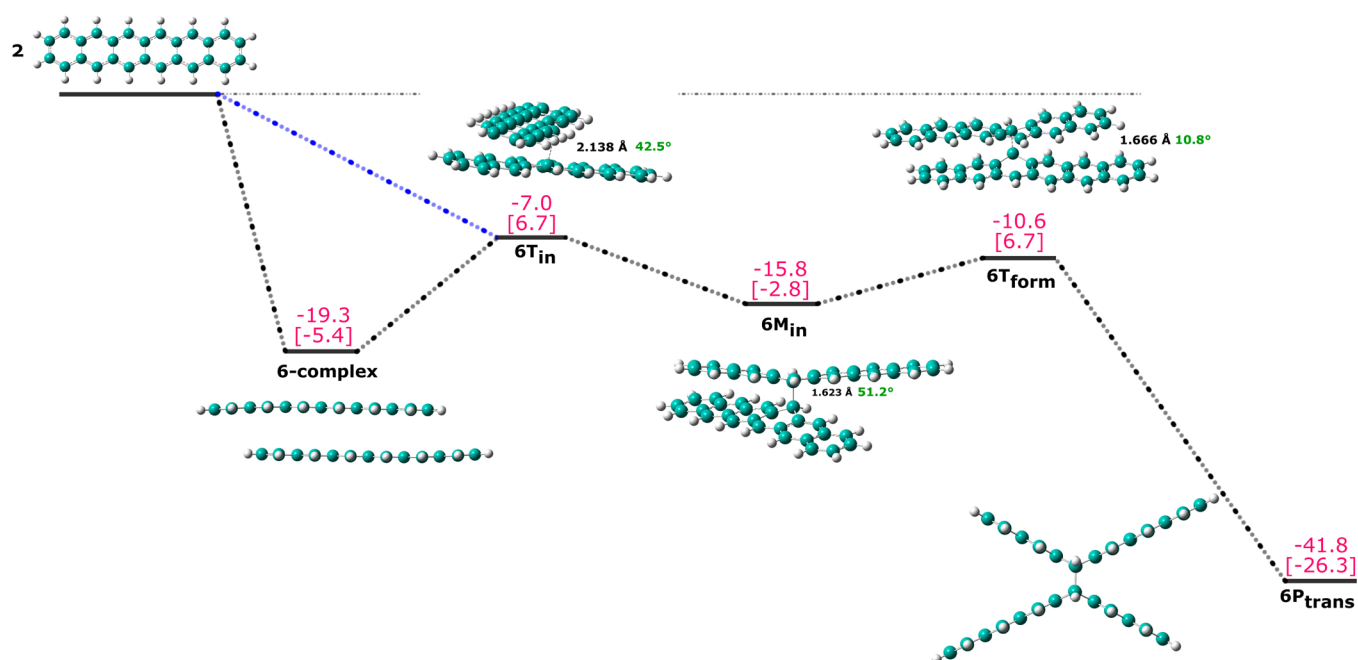


**Figure 6.** Reaction path for the dimerization of hexacene leading to an *trans*-product at the M06-2X/6-31G(d)+ZPVE level. Calculated energies (in kcal/mol, red), bond lengths (in Å, black), and dihedral angles (green) of newly forming C–C bonds (dashed lines between molecules) are shown. The Gibbs free energy ( $\Delta G$ , in kcal/mol) values are given in brackets.

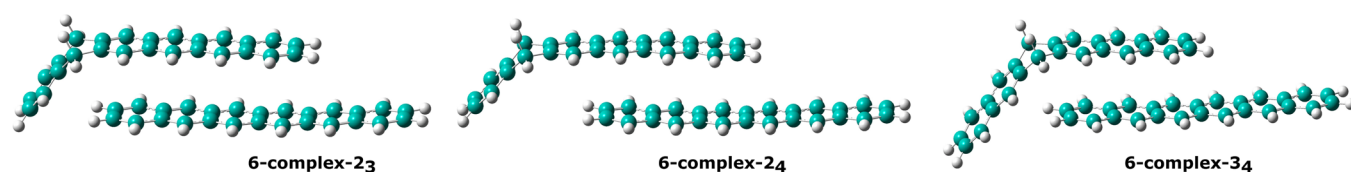


**Figure 7.** Different starting complexes for modeling hexacene polymerization at M06-2X/6-31G(d)+ZPVE.

without including ZPVE), which should be roughly multiplied by 2 to be compared with the formation of the polymer **poly-5P-2,2'** (which is 37.0 kcal/mol without including ZPVE, Table 1). However, formation of pentacene dimer **5P-3,3'** from two pentacene molecules is even more exothermic at -39.1 kcal/mol (without including of ZPVE, Table 1), so the formation of acene-based polymers from pentacene is not expected from both the kinetic and thermodynamic standpoints, since the competing dimerization reaction should be preferable.

**c. Dimerization of Hexacene.** In order to discuss hexacene polymerization, it is important to understand the mechanism for hexacene dimerization. However, the dimerization of hexacene was not studied previously, so we calculated the reaction pathway for hexacene dimerization in the current work (Table 2 and Figure 6).<sup>23</sup> The mechanism of hexacene dimerization is found to be similar to that of pentacene dimerization and differs from the dimerization mechanism of heptacene. The biradical mechanism for dimerization of hexacene proceeds via *syn* or *anti* transition states and biradical minima through stepwise biradical pathways, while dimerization of heptacene proceeds via asynchronous ring closure of the complex formed by two heptacene molecules.<sup>14</sup> Hexacene dimerization is calculated to have a negative activation energy (-7.0 kcal/mol) relative to two hexacene molecules at M06-2X/6-31G(d)+ZPVE. The unsubstituted hexacene is highly reactive in solution.<sup>2</sup> A dimerization reaction involving hexacene with relatively bulky substituents was reported even during storage in the solid state in the dark.<sup>12,24</sup> The formation

of a complex of two hexacene molecules, **6-complex**, is exothermic by 19.3 kcal/mol (related values for pentacene and heptacene complexes are -17.0 and -24.4 kcal/mol<sup>14</sup>). The formation of the **6-complex** is followed by an open shell transition state,  $6T_{in}$  ( $\langle S^2 \rangle = 0.31$ ), which is 7.0 kcal/mol lower in energy than the reactants and 12.3 kcal/mol higher than the **6-complex**. The transition state  $6T_{in}$  leads to the minimum  $6M_{in}$  ( $\langle S^2 \rangle = 1.00$ ), which is 15.8 kcal/mol more stable than the reactants. The pathway from  $6M_{in}$  to  $6P_{trans}$  via  $6T_{form}$  ( $6T_{form}$  is 10.6 kcal/mol lower in energy than two hexacene molecules and has  $\langle S^2 \rangle = 0.64$ ), requires an activation energy of only 5.2 kcal/mol relative to  $6M_{in}$  and the resulting dimer is 41.8 kcal/mol more stable than the starting materials (Figure 6, for comparison, the pentacene dimer is 34.3 kcal/mol and the heptacene dimer is 49.1 kcal/mol more stable than the corresponding starting materials<sup>14</sup>).

**d. Polymerization of Hexacene.** For the polymerization of hexacene, we considered all three energetically reasonable pathways. These pathways proceed via one of three complexes whose formation is exothermic by 17.2 (**6-complex-2<sub>3</sub>**), 12.5 (**6-complex-2<sub>4</sub>**), and 14.2 kcal/mol (**6-complex-3<sub>4</sub>**) (Figures 7–10 and Table 2). **6-Complex-2<sub>3</sub>** can be compared with a complex between a tetracene and a hexacene molecules, in which overlap can be expected between only four benzene rings. The extra stabilization can be attributed to herringbone-type interactions between the bent segment of the polymer's terminal unit and the newly binding acene molecule. Polymerization starting from **6-complex-2<sub>3</sub>** (Figure 8) leads to **poly-6P-**

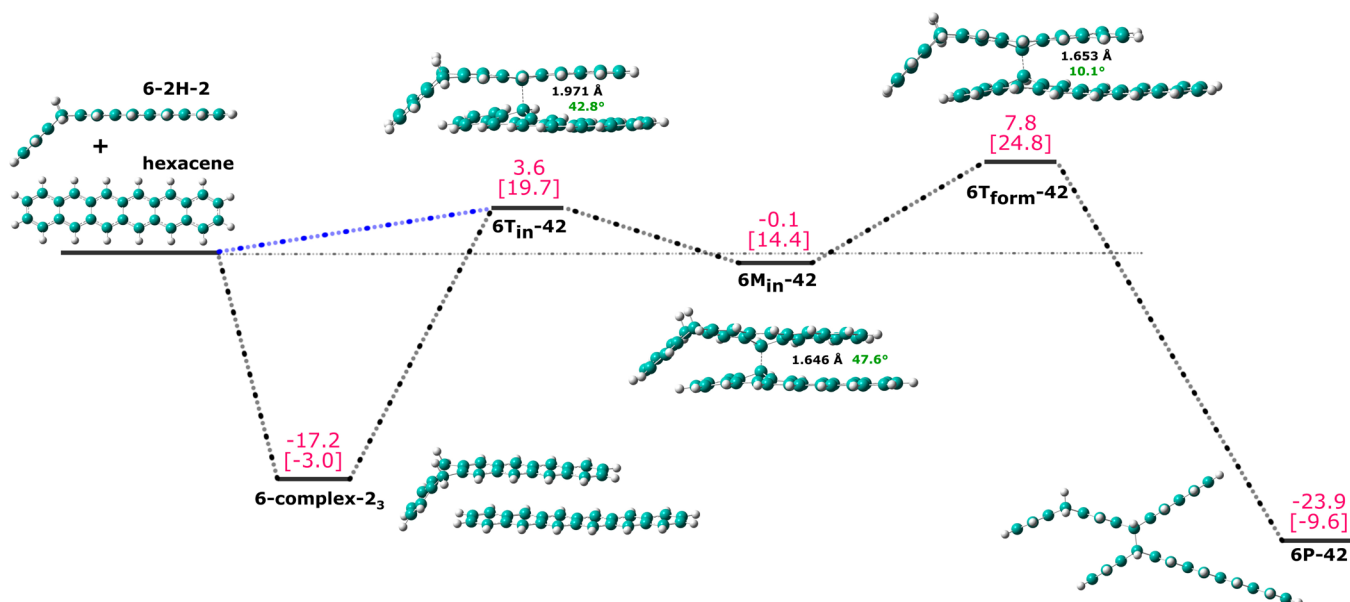


**Figure 8.** Reaction path for a propagation step in hexacene polymerization starting from **6-complex-2<sub>3</sub>** at M06-2X/6-31G(d)+ZPVE. This reaction should lead to formation of the polymer **poly-6P-2,3'** (Figure 4). Calculated energies (in kcal/mol, red), bond lengths (in Å, black), and dihedral angles (green) of newly forming C–C bonds (dash lines between molecules) are shown. The Gibbs free energy ( $\Delta G$ , in kcal/mol) values are given in brackets.

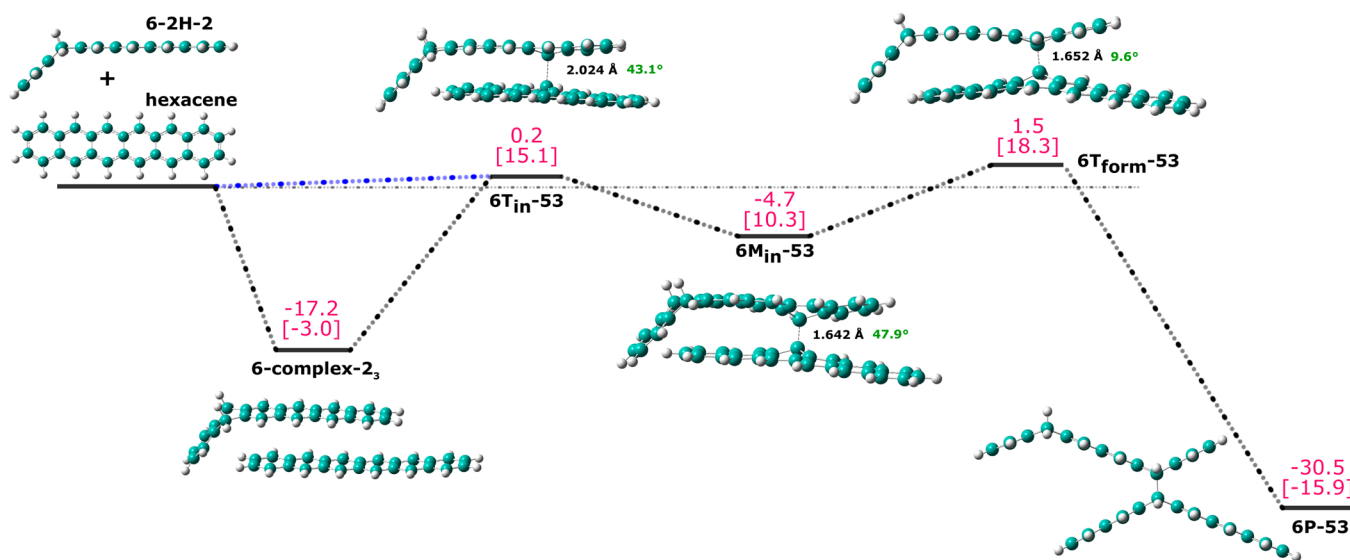


**Figure 9.** Reaction path for a propagation step in hexacene polymerization starting from **6-complex-2<sub>3</sub>** (Figure 4) at M06-2X/6-31G(d)+ZPVE. Calculated energies (in kcal/mol, red), bond lengths (in Å, black) and dihedral angles (green) of newly forming C–C bonds (dash lines between molecules) are shown. The Gibbs free energy ( $\Delta G$ , in kcal/mol) values are given in brackets.<sup>25</sup>

**2,3'** (Figure 4), while polymerization starting from **6-complex-2<sub>4</sub>** (Figure 10) leads to the formation of **poly-6P-2,2'** (Figure 4). The reaction proceeding via **6-complex-3<sub>4</sub>** is kinetically unfavorable because the reaction is equivalent to one between anthracene and the second ring of hexacene, and so it would require a relatively high activation energy of about 20–30 kcal/mol based on data available below in this paper and in ref 14. Therefore, we did not further investigate the mechanistic pathway originating from **6-complex-3<sub>4</sub>**.

Starting from **6-complex-2<sub>3</sub>** (Figures 8 and 9), we considered pathways via transition states **6T<sub>in</sub>-42** and **6T<sub>in</sub>-53**, respectively, while starting from **6-complex-2<sub>4</sub>** (Figure 10), we considered a pathway via transition state **6T<sub>in</sub>-52**. The activation energies for **6T<sub>in</sub>-42**, **6T<sub>in</sub>-53**, and **6T<sub>in</sub>-52** are 3.6, 0.2, and 6.3 kcal/mol,

respectively, compared with the starting materials hexacene and **6-2H-2**. The activation energies of **T<sub>in</sub>** starting from the corresponding complexes are 20.8, 17.4, and 18.8 kcal/mol, respectively. **6T<sub>in</sub>-52** has a higher activation energy than the other two transition states (relative to the starting materials). Forming C–C bond lengths are 1.97, 2.02, and 2.00 Å, and the dihedral angles between the forming C–C bonds are 42.8, 43.1, and 51.3° for **6T<sub>in</sub>-42**, **6T<sub>in</sub>-53**, and **6T<sub>in</sub>-52**, respectively. The spin contamination values ( $\langle S^2 \rangle = 0.35, 0.43, \text{ and } 0.64$  for **6T<sub>in</sub>-42**, **6T<sub>in</sub>-53**, and **6T<sub>in</sub>-52**) indicate the biradical nature of the **6T<sub>in</sub>** transition states.

From transition states **T<sub>in</sub>**, the reactions proceed to minima **6M<sub>in</sub>-42**, **6M<sub>in</sub>-53**, and **6M<sub>in</sub>-52** (Figures 8–10), which have energies of -0.1, -4.7, and 1.7 kcal/mol, respectively,

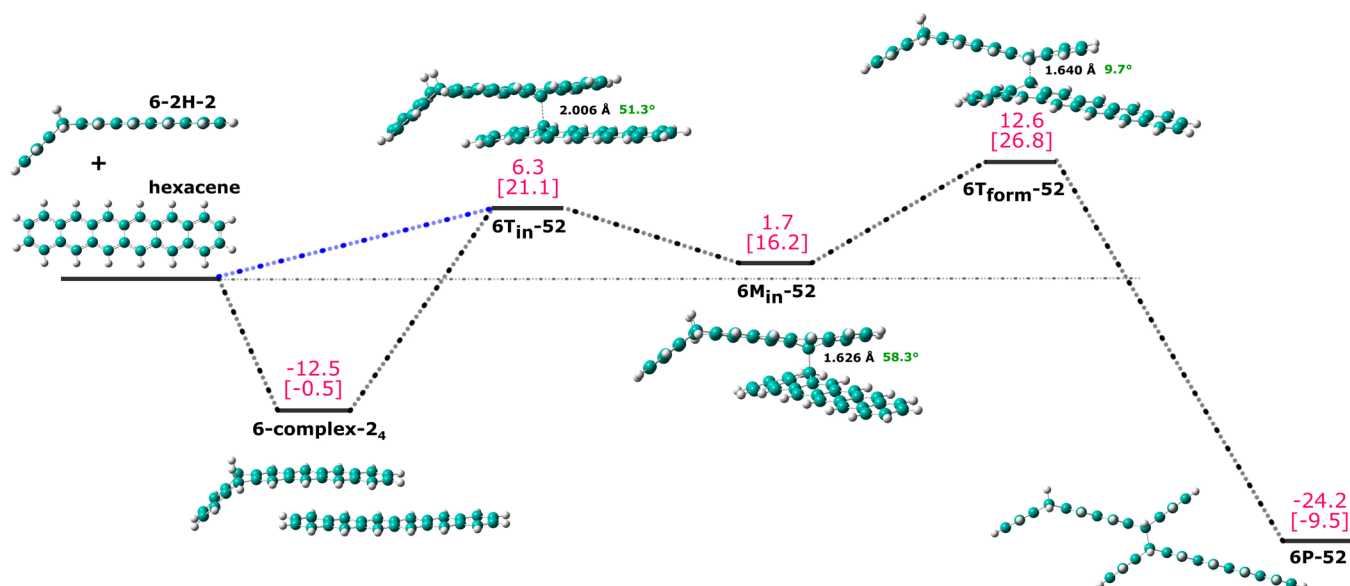


**Figure 10.** Reaction path for a propagation step in hexacene polymerization starting from 6-complex-2<sub>4</sub> at M06-2X/6-31G(d)+ZPVE. This reaction should lead to formation of the polymer poly-6P-2,2' (Figure 4). Calculated energies (in kcal/mol, red), bond lengths (in Å, black) and dihedral angles (green) of newly forming C–C bonds (dash lines between molecules) are shown. The Gibbs free energy ( $\Delta G$ , in kcal/mol) values are given in brackets.

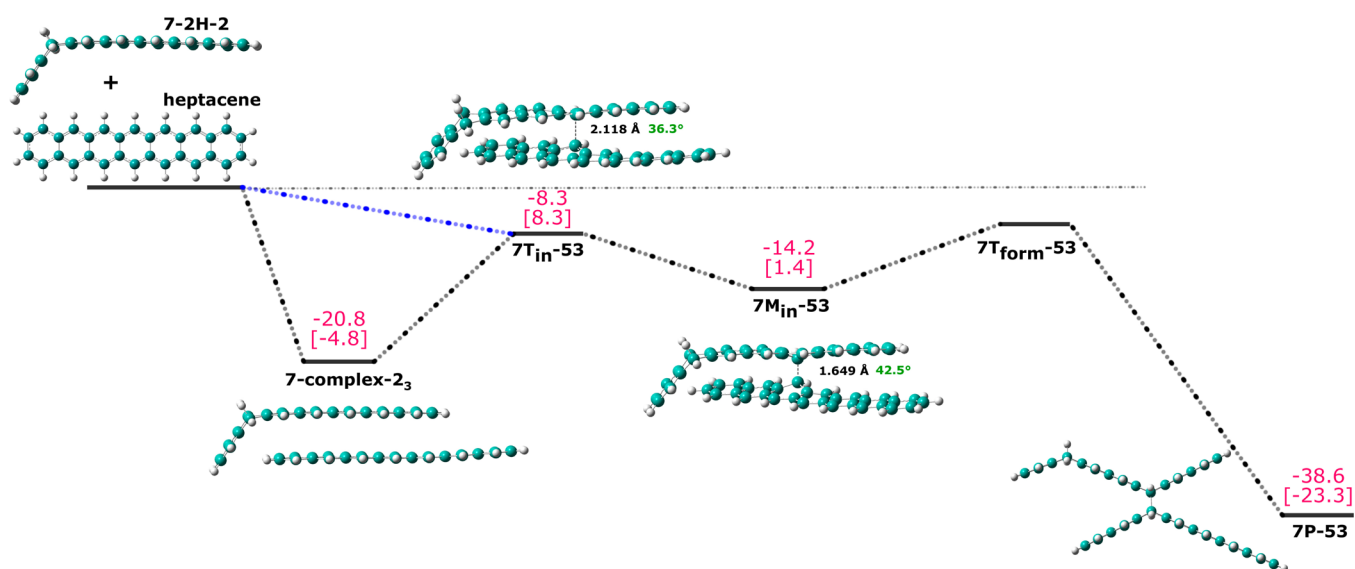


**Figure 11.** Reaction path for a propagation step in heptacene polymerization starting from 7-complex-2<sub>3</sub> at M06-2X/6-31G(d)+ZPVE. This reaction should lead to formation of the polymer poly-7P-2,3' (Figure 4). Calculated energies (in kcal/mol, red), bond lengths (in Å, black) and dihedral angles (green) of newly forming C–C bonds (dash lines between molecules) are shown. The Gibbs free energy ( $\Delta G$ , in kcal/mol) values are given in brackets.

compared with the initial hexacene and 6-2H-2. These minima 6M<sub>in</sub>-42, 6M<sub>in</sub>-53, and 6M<sub>in</sub>-52 (spin contamination of  $\langle S^2 \rangle = 0.96, 0.96, \text{ and } 1.05$ , respectively) are 3.7, 4.9, and 4.6 kcal/mol, respectively, lower in energy than the corresponding T<sub>in</sub> transition states. The reactions further proceed to form the products via rate-determining transition states of the T<sub>form</sub> type, 6T<sub>form</sub>-42, 6T<sub>form</sub>-53, and 6T<sub>form</sub>-52 having spin contaminations of  $\langle S^2 \rangle = 0.67, 0.75, \text{ and } 0.77$  and activation energies of 7.8, 1.5, and 12.6 kcal/mol, respectively, compared with the starting hexacene and 6-2H-2. Overall, the activation energies of T<sub>form</sub> transition states are slightly lower than the values expected on the basis of the number of aromatic rings because of the presence of the additional herringbone-type interaction.

The activation energy for the kinetically most preferred propagation step of hexacene polymerization is 1.5 kcal/mol (Figure 9), however, this propagation step might not lead to the most preferred polymerization mechanism<sup>25</sup> and the expected lowest activation energy for polymerization of hexacene (based on the propagation step in Figure 8) is 7.8 kcal/mol. This activation energy for hexacene polymerization is higher than the activation energy for hexacene dimerization (−7.0 kcal/mol, Table 2 and Figure 6).

*e. Polymerization of Heptacene.* Overall, the mechanism of heptacene polymerization is very similar to those of hexacene and pentacene polymerization. Possible pathways for the propagation step in the polymerization of heptacene are



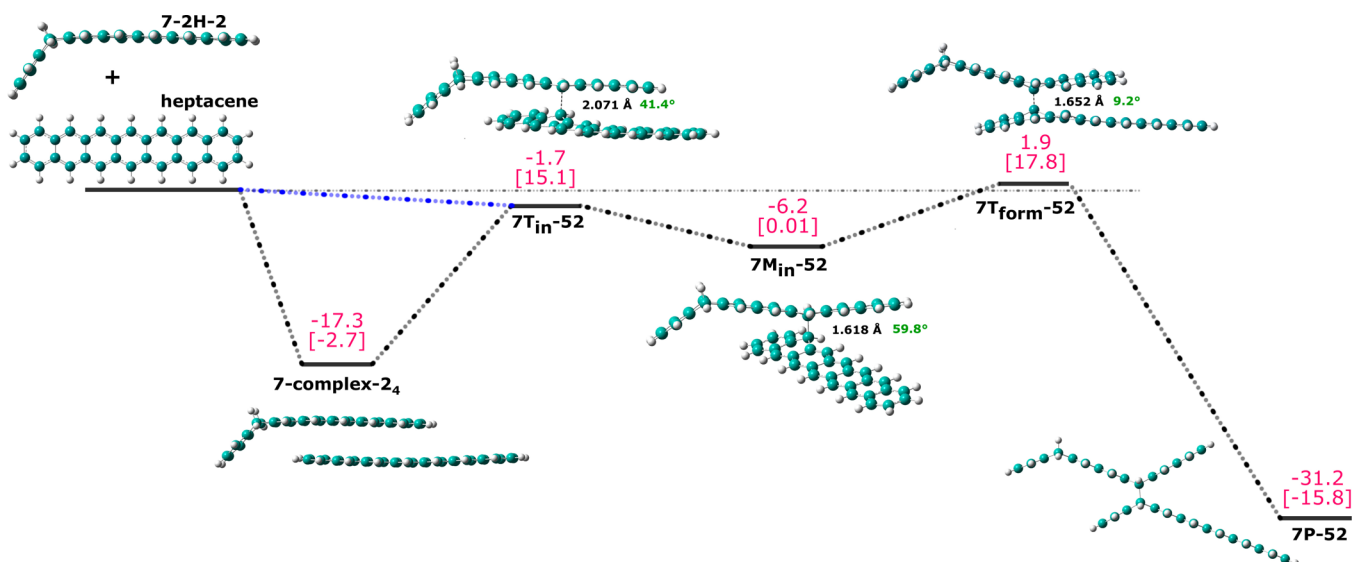


**Figure 12.** Reaction path for a propagation step in heptacene polymerization starting from 7-complex-2<sub>4</sub> at M06-2X/6-31G(d)+ZPVE. This reaction should lead to formation of the polymer poly-7P-2,3' (Figure 4). Calculated energies (in kcal/mol, red), bond lengths (in Å, black), and dihedral angles (green) of newly forming C–C bonds (dash lines between molecules) are shown. The Gibbs free energy (ΔG, in kcal/mol) values are given in brackets.

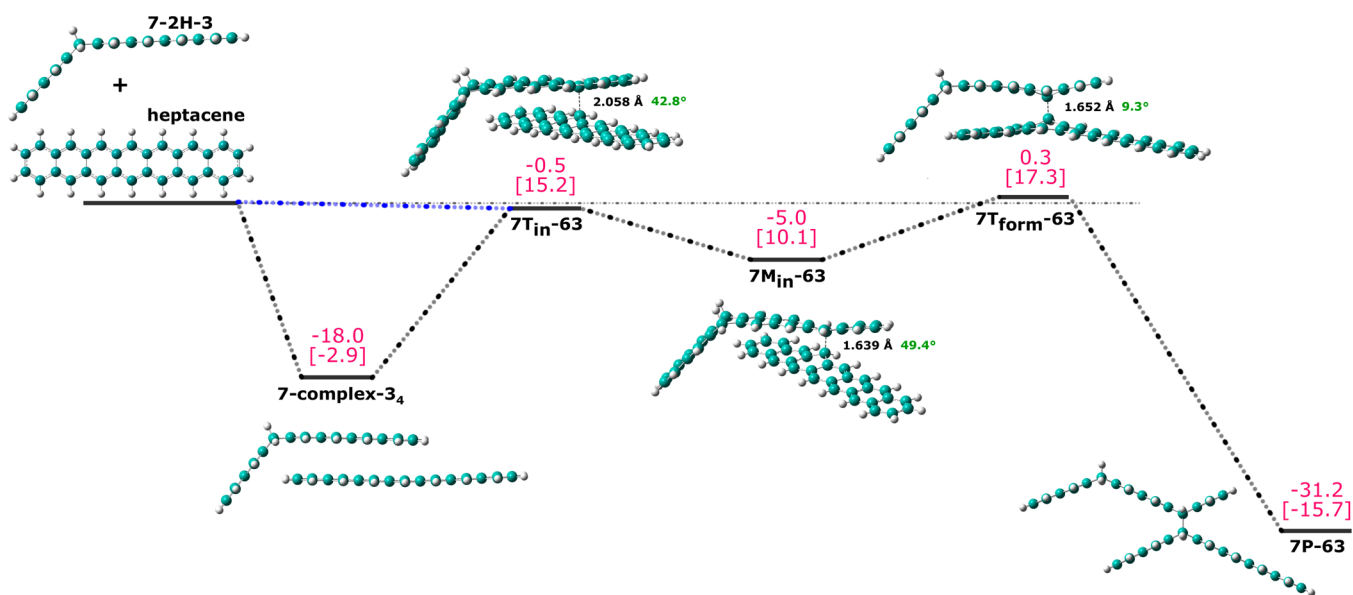


**Figure 13.** Reaction path for a propagation step in heptacene polymerization starting from 7-complex-3<sub>4</sub> at M06-2X/6-31G(d)+ZPVE. This reaction should lead to formation of the polymer poly-7P-2,3' (Figure 4). Calculated energies (in kcal/mol, red), bond lengths (in Å, black), and dihedral angles (green) of newly forming C–C bonds (dash lines between molecules) are shown. The Gibbs free energy (ΔG, in kcal/mol) values are given in brackets.

shown in Figures 11–13, and the corresponding energies are given in Table 2. The  $\pi$ -complex can be formed through the terminal heptacene moiety in the forming polymer and the approaching heptacene molecule, which we have modeled by considering 7-complex-2<sub>3</sub>, 7-complex-2<sub>4</sub>, and 7-complex-3<sub>4</sub> (Figures 11–13). Interestingly, considering steric factors, all the energetically reasonable pathways for polymer formation starting from these three complexes result in the formation of the same polymer, poly-7P-2,3' (Figure 4, the formed polymers will differ only in terms of the identity of the first heptacene moiety in the resulting polymer). The formations of 7-complex-2<sub>3</sub>, 7-complex-2<sub>4</sub>, and 7-complex-3<sub>4</sub> are exothermic by 20.8, 17.3, and 18.0 kcal/mol, respectively. Originating from

these three complexes, we have considered three transition states 7T<sub>in</sub>-53, 7T<sub>in</sub>-52, and 7T<sub>in</sub>-63. These transition states have spin contaminations of  $\langle S^2 \rangle = 0.52, 0.65,$  and  $0.58,$  respectively, and activation energies of  $-8.3, -1.7,$  and  $-0.5,$  respectively, relative to the reactants (i.e., the heptacene and 7-2H-2 or 7-2H-3 molecules; the activation energies are 12.5, 15.6, and 17.5 kcal/mol, respectively, relative to the corresponding complexes). The reaction proceeds from the T<sub>in</sub> transition states to the intermediates, 7M<sub>in</sub>-53, 7M<sub>in</sub>-52, and 7M<sub>in</sub>-63, which are lower in energy than the starting materials by 14.2, 6.2, and 5.0 kcal/mol, respectively. From the intermediates, the rate-determining transition states, 7T<sub>form</sub>-52 and 7T<sub>form</sub>-63 (Figures 12 and 13), lead to product formation

and have activation energies of 1.9 and 0.3 kcal/mol relative to the reactants (19.2 and 18.3 kcal/mol relative to the corresponding complexes).<sup>26</sup> Therefore, overall the expected activation energy for polymerization of heptacene is somewhat below zero kcal/mol (relative to the reactants).<sup>26</sup> For comparison, the activation energy for the corresponding heptacene dimerization is  $-12.1$  kcal/mol relative to two heptacene molecules and is  $+12.3$  kcal/mol relative to the complex formed between two heptacene molecules.<sup>14</sup>

#### f. General Discussion of the Polymerization Mechanism.

The activation energy for the formation of acene-based polymers is higher than for the formation of acene dimers, since cycloaddition in the polymerization reactions does not occur at the central acene ring. However, polymerization of heptacene (and, clearly, of longer acenes) is barrierless relative to the reactants. During acene polymerization, the preferred disposition of the approaching acene molecule over the terminal acene unit of the forming polymer is limited to an overlap of, at most, two-thirds of the length of each acene (because of the presence, roughly one-third of the way along the terminal acene, of  $sp^3$ -hybridized carbon atoms from previous propagation steps). Consequently, polymerization proceeds via reaction with only a segment of the terminal acene unit, with the reactivity of this segment being equivalent to that of an acene two-thirds its initial length. In the hypothetical case of a gas-phase reaction, for acenes of any length, dimerization will always be kinetically more favorable than polymerization (see Table 2), while in solution, for long acenes, both polymerization and dimerization will be very fast processes. Also, for long acenes, acene based polymers are thermodynamically controlled products, since four new C–C bonds are formed on each acene molecule during polymerization. Based on the results in Table 1, from a thermodynamic point of view, polymerization rather than dimerization can be expected in the case of hexacene and heptacene. Although hexacene dimerization is thermodynamically less favorable by 9.1 kcal/mol than the formation of the most stable hexacene-based polymer, from a kinetic point of view, formation of hexacene-based polymers might not occur because of the higher activation energy for polymerization vs dimerization. For heptacene, the formation of a heptacene-based polymer is more likely.

The dimerization reactions discussed here should have a second-order reaction kinetics. Polymerization should have first order reaction kinetics considering that the formed polymer backbone is completely insoluble in organic solvents and forms a solid precipitate. Therefore, the tendency to form a dimer or a polymer may depend on the concentration of the reacting acene. For example, as we discussed above, although hexacene dimerization is preferred kinetically by about 8.5 kcal/mol, this preference will vanish if the concentration of the monomer is  $10^{-6}$  M (bearing in mind that the solubility of long acenes is very low<sup>2a</sup>).

## CONCLUSIONS

In this paper, we have explored the structure, mechanism (kinetics), and thermodynamics of acene-based polymer formation using computational methods. Experimentally, dimerization and polymerization products of long acenes are very difficult to characterize, although this study suggests that acene based polymers or their fragments were possibly obtained by the Neckers and Bettinger groups.<sup>5e</sup> For hexacene and heptacene, we have considered the formation of various

possible acene-based polymers, which were calculated to be thermodynamically preferred over the dimerization products and have low activation energies for polymer formation. Thus, polymerization can be expected to compete with dimerization in the case of hexacene and heptacene (and especially for longer acenes). Similarly to dimerization, the polymerization of acenes follows a stepwise biradical pathway. For steric reasons, the polymerization of acenes cannot proceed through an *anti*-type transition state because the rotation after an *anti*-transition state is rendered impossible by the bent nature of the participating acene unit of the forming polymer. More importantly, polymerization of acenes proceeds via reaction of only a segment of the terminal acene unit, with this segment being shorter, and therefore less reactive, than the pristine acene molecule, so for acenes of any length, dimerization will always be kinetically more favorable than polymerization. However, polymerization of long acenes (starting from heptacene) should be barrierless (relative to the reactants) and both polymerization and dimerization should be very fast processes for long acenes. Since dimerization is a second-order reaction, while polymerization is a first-order reaction, competition between polymerization and dimerization should be concentration dependent, and at low acene concentrations, polymerization will be preferred.

## ASSOCIATED CONTENT

### Supporting Information

Calculated absolute energies for all reactants, products, and intermediates mentioned in the paper as well as the coordinates of their optimized structures. Full citation of ref 16. This material is available free of charge via the Internet at <http://pubs.acs.org>.

## AUTHOR INFORMATION

### Corresponding Authors

\*E-mail: (S.S.Z.) [sanjiozade@iiserkol.ac.in](mailto:sanjiozade@iiserkol.ac.in).

\*E-mail: (N.Z.) [natalia.zamoshchik@weimann.ac.il](mailto:natalia.zamoshchik@weimann.ac.il).

### Notes

The authors declare no competing financial interest.

## ACKNOWLEDGMENTS

We thank Dr. Denis Sheberla for useful discussions and the MINERVA Foundation and the Israel Science Foundation for financial support.

## DEDICATION

§Dedicated to our friend and devoted teacher, Prof. Michael Bendikov, who passed away on July 2, 2013.

## REFERENCES

- (1) (a) Clar, E. *Polycyclic Hydrocarbons*; Academic Press: London, 1964; Vols. 1 and 2. (b) Havey, R. G. *Polycyclic Aromatic Hydrocarbons*; Wiley-VCH: New York, 1997. (c) Geerts, Y.; Klärner, G.; Müllen, K. In *Electronic Materials: The Oligomer Approach*, Müllen, K., Wagner, G., Eds.; Wiley-VCH: Weinheim, 1998; p 48.
- (2) (a) Bendikov, M.; Wudl, F.; Perepichka, D. F. *Chem. Rev.* **2004**, *104*, 4891. (b) Anthony, J. E. *Chem. Rev.* **2006**, *106*, 5028–5048. (c) Anthony, J. E. *Angew. Chem., Int. Ed.* **2008**, *47*, 452–483.
- (3) (a) Mallick, A. B.; Locklin, J.; Mannsfeld, S. C. B.; Reese, C.; Robert, M. E.; Senatore, M. L.; Zi, H.; Bao, Z. In *Organic Field-Effect Transistor*; Locklin, J., Bao, Z., Eds.; CRC Press: Boca Raton, 2007; Section 3.2, pp 159–228. (b) Meng, H.; Bendikov, M.; Mitchell, G.; Helgeson, R.; Wudl, F.; Bao, Z.; Siegrist, T.; Kloc, C.; Chen, C.-H.

*Adv. Mater.* **2003**, *15*, 1090–1093. (c) Murphy, A. R.; Fréchet, J. M. J. *Chem. Rev.* **2007**, *107*, 1066–1096. (d) Park, S. K.; Jackson, T. N.; Anthony, J. E.; Mourey, D. A. *Appl. Phys. Lett.* **2007**, *91*, 063514/1–3. (e) Smith, J.; Zhang, W.; Sougrat, R.; Zhao, K.; Li, R.; Cha, D.; Amassian, A.; Heeney, M.; McCulloch, I.; Anthopoulos, T. D. *Adv. Mater.* **2012**, *24*, 2441–2446.

(4) Zade, S. S.; Bendikov, M. *Angew. Chem., Int. Ed.* **2010**, *49*, 4012–4015.

(5) (a) Payne, M. M.; Parkin, S. R.; Anthony, J. E. *J. Am. Chem. Soc.* **2005**, *127*, 8028–8029. (b) Mondal, R.; Shah, B. K.; Neckers, D. C. *J. Am. Chem. Soc.* **2006**, *128*, 9612–9613. (c) Chun, D.; Cheng, Y.; Wudl, F. *Angew. Chem., Int. Ed.* **2008**, *47*, 8380–8385. (d) Kaur, I.; Stein, N. N.; Kopeski, R. P.; Miller, G. P. *J. Am. Chem. Soc.* **2009**, *131*, 3424–3425. (e) Mondal, R.; Tönshoff, C.; Khon, D.; Neckers, D. C.; Bettinger, H. F. *J. Am. Chem. Soc.* **2009**, *131*, 14281–14289. (f) Purushothaman, B.; Bruzek, M.; Parkin, S. R.; Miller, A.-F.; Anthony, J. E. *Angew. Chem., Int. Ed.* **2011**, *50*, 7013–7017. (g) Watanabe, M.; Chang, Y. J.; Liu, S.-W.; Chao, T.-H.; Goto, K.; Islam, M. M.; Yuan, C.-H.; Tao, Y.-T.; Shinmyozu, T.; Chow, T. J. *Nature Chem.* **2012**, *4*, 574–578. (h) Xiao, J.; Duong, H. M.; Liu, Y.; Shi, W.; Ji, L.; Li, G.; Li, S.; Liu, X.-W.; Ma, J.; Wudl, F.; Zhang, Q. *Angew. Chem., Int. Ed.* **2012**, *51*, 6094–6098. (i) Mondal, R.; Adhikari, R. M.; Shah, B. K.; Neckers, D. C. *Org. Lett.* **2007**, *9*, 2505.

(6) (a) Kaur, I.; Jazdzzyk, M.; Stein, N. N.; Prusevich, P.; Miller, G. P. *J. Am. Chem. Soc.* **2010**, *132*, 1261–1263. (b) Tönshoff, C.; Bettinger, H. F. *Angew. Chem., Int. Ed.* **2010**, *49*, 4125–4128.

(7) Watanabe, M.; Su, W.-T.; Chen, K.-Y.; Chien, C.-T.; Chao, T.-H.; Chang, Y. J.; Liue, S.-W.; Chow, T. J. *Chem. Commun.* **2013**, *49*, 2240–2242.

(8) For a review of computational studies on acene reactivity, see: Zade, S. S.; Bendikov, M. *J. Phys. Org. Chem.* **2012**, *25*, 452–461.

(9) For a review of the dependence of different electronic properties of conjugated systems on chain length, see: Zade, S. S.; Zamoshchik, N.; Bendikov, M. *Acc. Chem. Res.* **2011**, *44*, 14–24.

(10) (a) Schönberg, A. *Preparative Organic Photochemistry*; Springer-Verlag: Berlin, 1968; p 99. (b) Bouas-Laurent, H.; Desvergne, J.-P. In *Photochromism, Molecules and Systems, revised*; Dürr, H., Bouas-Laurent, H., Eds.; Elsevier: New York, 2003; Chapter 14. (c) Yamamoto, S.; Grellman, K. H. *Chem. Phys. Lett.* **1982**, *92*, 533–540.

(11) (a) Bouas-Laurent, H.; Castellan, A.; Desvergne, J.-P.; Lapouyade, R. *Chem. Soc. Rev.* **2000**, *29*, 43–55. (b) Bouas-Laurent, H.; Castellan, A.; Desvergne, J.-P.; Lapouyade, R. *Chem. Soc. Rev.* **2001**, *30*, 248–263. (c) Becker, H. D. *Chem. Rev.* **1993**, *93*, 145–172.

(12) Purushothaman, B.; Parkin, S. R.; Anthony, J. E. *Org. Lett.* **2010**, *12*, 2060–2063.

(13) Perepichka, D. F.; Bendikov, M.; Meng, H.; Wudl, F. *J. Am. Chem. Soc.* **2003**, *125*, 10190.

(14) Zade, S. S.; Zamoshchik, N.; Reddy, A. R.; Fridman-Marueli, G.; Sheberla, D.; Bendikov, M. *J. Am. Chem. Soc.* **2011**, *133*, 10803–10816.

(15) Fang, T. *Heptacene, Octacene, Nonacene, Supercene and Related Polymers*, Ph.D. Dissertation, University of California, Los Angeles, CA, 1986.

(16) Frisch, M. J. et al. *Gaussian 09, revision A.02*; Gaussian, Inc.: Wallingford, CT, 2009.

(17) (a) Parr, R. G.; Yang, W. *Density-Functional Theory of Atoms and Molecules*; Oxford University Press: New York, 1989. (b) Koch, W.; Holthausen, M. C. *A Chemist's Guide to Density Functional Theory*; Wiley-VCH: New York, 2000.

(18) Zhao, Y.; Truhlar, D. G. *Theor. Chem. Acc.* **2008**, *120*, 215–241.

(19) (a) Gonzalez, C.; Schlegel, H. B. *J. Chem. Phys.* **1989**, *90*, 2154. (b) Gonzalez, C.; Schlegel, H. B. *J. Chem. Phys.* **1990**, *94*, 5523.

(20) (a) Kudin, K. N.; Scuseria, G. E. *Chem. Phys. Lett.* **1998**, *289*, 611. (b) Kudin, K. N.; Scuseria, G. E. *Phys. Rev. B* **2000**, *61*, 16440.

(21) The validity of using the hydrogen-terminated acene unit as a model for the reacting polymer in the propagation step was tested by using a hydrogen-terminated acene dimer in the propagation step of pentacene polymerization (Figure 5 and Figure S1, Supporting Information). Enlarging the model by an additional acene unit leads

to only very minor changes in the energies and structure of the potential energy surface.

(22) The  $\Delta E$  and  $\Delta\Delta E$  values for **poly-6P-2,3'** reported in Table 2 of ref 14 contain a typographical error and are incorrect. The energy of **poly-6P-2,3'** is not discussed in ref. 14.

(23) The mechanism leading to the most stable *trans*-product was calculated in this work.

(24) Acenes (such as pentacene and hexacene) are known to exhibit tight packing.<sup>2,5f</sup> Consequently, in the solid state longer acenes including hexacene are significantly more stable than in solution because the planar structure of acene needs to bend strongly to form the dimerization or polymerization product.<sup>14</sup>

(25) The reaction of **6P-53** (Figure 9) with the next hexacene molecule will be different from the pathway presented in Figure 9 and similar, from a kinetic point of view, to reaction between an anthracene moiety and the second ring of hexacene (and similar to the reactivity of complex **6-complex-3<sub>4</sub>**). Such a reaction should have a high activation energy and lead to **poly-6P-2,3'-alt-2,2'** (Figure 4). Thus, the polymerization reaction that proceeds via **6P-53** and begins with the propagation step as in Figure 9 will require an activation energy that is significantly higher than that of the pathway presented in Figure 9.

(26) Generally,  $T_{\text{form}}$  has a very flat potential energy surface in all of the cases studied in Figures 5, 6, and 8–13, and we were not able to locate transition state  $7T_{\text{form}}-53$  despite numerous attempts. About 10 different starting geometries were tried. In some cases, force constants were recalculated at each optimization step, an ultrafine internal grid was used, and the QST3 transition state search algorithm was applied. Based on the energies given in Figures 8–13, we expect the energy of  $7T_{\text{form}}-53$  to be 5–10 kcal/mol lower than that of  $7T_{\text{form}}-52$  and  $7T_{\text{form}}-63$  (1.9 and 0.3 kcal/mol, respectively) and slightly higher than that of  $7T_{\text{in}}-53$ , whose energy is  $-8.3$  kcal/mol.